11. V. Tsatourian, H. S. Margolis, G. Marra, D. T. Reid, and P. Gill, "Common-path self-referencing interferometer for carrier-envelope offset frequency stabilization with enhanced noise immunity," Opt. Lett. **35**(8), 1209–1211 (2010).
12. C. Grebing, S. Koke, B. Manschwetus, and G. Steinmeyer, "Performance comparison of interferometer topologies for carrier-envelope phase detection," Appl. Phys. B **95**(1), 81–84 (2009).
13. S. Rausch, T. Binhammer, A. Harth, E. Schulz, M. Siegel, and U. Morgner, "Few-cycle oscillator pulse train with constant carrier-envelope- phase and 65 as jitter," Opt. Express **17**(22), 20282–20290 (2009).
14. E. B. Kim, J. H. Lee, L. T. Trung, W.-K. Lee, D.-H. Yu, H. Y. Ryu, C. H. Nam, and C. Y. Park, "Demonstration of an optical frequency synthesizer with zero carrier-envelope-offset frequency stabilized by the direct locking method," Opt. Express **17**(23), 20920–20926 (2009).
15. J.-H. Lee, Y. S. Lee, J. Park, T. J. Yu, and C. H. Nam, "Long-term carrier-envelope-phase stabilization of a femtosecond laser by the direct locking method," Opt. Express **16**(17), 12624–12631 (2008).
16. C. Yun, S. Chen, H. Wang, M. Chini, and Z. Chang, "Temperature feedback control for long-term carrier-envelope phase locking," Appl. Opt. **48**(27), 5127–5130 (2009).
17. T. M. Fortier, A. Bartels, and S. A. Diddams, "Octave-spanning Ti:sapphire laser with a repetition rate >1 ghz for optical frequency measurements and comparisons," Opt. Lett. **31**(7), 1011–1013 (2006).
18. T. Fuji, J. Rauschenberger, A. Apolonski, V. S. Yakovlev, G. Tempea, Th. Udem, C. Gohle, T. W. Hänsch, W. Lehnert, M. Scherer, and F. Krausz, "Monolithic carrier-envelope phase-stabilization scheme," Opt. Lett. **30**(3), 332–334 (2005).
19. L.-J. Chen, A. J. Benedick, J. R. Birge, M. Y. Sander, and F. X. Kärtner, "Octave-spanning, dual-output 2.166 GHz Ti:sapphire laser," Opt. Express **16**(25), 20699–20705 (2008).
20. D. A. Howe, D. W. Allan, and J. A. Barnes, "Properties of signal sources and measurement methods," Proceedings of the 35th Annual Symposium on Frequency Control (1981).
21. J. Rutman, and F. L. Walls, "Characterization of frequency stability in precision frequency sources," Proc. IEEE **79**(7), 952–960 (1991).
22. S. T. Cundiff, and J. Ye, "Phase stabilization of mode-locked lasers," J. Mod. Opt. **52**(2), 201–219 (2005).
23. T. M. Fortier, D. J. Jones, J. Ye, S. T. Cundiff, and R. S. Windeler, "Long-term carrier-envelope phase coherence," Opt. Lett. **27**(16), 1436–1438 (2002).
24. T. M. Fortier, J. Ye, S. T. Cundiff, and R. S. Windeler, "Nonlinear phase noise generated in air-silica microstructure fiber and its effect on carrier-envelope phase," Opt. Lett. **27**(6), 445–447 (2002).

1. Introduction

Long-term carrier-envelope phase (CEP) coherence of few-cycle lasers plays an important role in coherent pulse synthesis [1], high-harmonic generation [2], and in the attosecond electron dynamics [3,4]. The pulse-to-pulse change of CEP ($\Delta\varphi$) in a femtosecond laser arises from the difference between group and phase velocities inside the laser cavity and varies rapidly over time. The precise measurement of CEP in successive laser pulses is essential for accurate control of CEP. A number of methods to measure CEP have been demonstrated in the time and frequency domains [5–9]. To detect CEP, the *f*-2*f* self-referencing technique is frequently used in a two-arm interferometer setup. The two-arm interferometer scheme, however, is vulnerable to environmental perturbations such as air fluctuation, mechanical vibration, and acoustic noise, because it has long arms with uncommon paths. Such noise elements generate phase drift and large accumulated phase slip, which prevents long-term CEP coherence. To avoid this noise issue, a He-Ne laser can be added to the two-arm interferometer to stabilize the interference fringes by feedback control [10]. This method can minimize the degrade effect of interferometer alignment; however, it also adds complexity to system. Another solution is to use a common-path interferometer or a collinear self-referencing setup [11–13]. This technique is clearly less sensitive to environmental variations and can minimize the interferometer setup as well. This benefit can allow improvements in stability and in long-term CEP coherence. Hence, several successful methods have been reported improved CEP stabilization [11–13].

Several attempts have been made as well to formulate a constant CEP, as laser pulses with identical pulse-to-pulse CEP values can be advantageous in certain applications [4,7]. With the generation of laser pulses with identical CEP values, a pulse selection scheme to choose pulses with same CEP is not necessary in field-sensitive experiments [2]. In addition the optical frequency measurement can be made simpler as the carrier-envelope-offset frequency is automatically set to zero [14]. It is, however, difficult to produce laser pulses directly with a constant CEP value, as the error signal becomes an even function near zero frequency. This can be solved by adding an acousto-optic modulator (AOM) to an *f*-2*f* interferometer to give the comb frequency pre-shift at the same frequency used for CEP stabilization but with an

#136419 - $15.00USD Received 11 Oct 2010; revised 24 Nov 2010; accepted 28 Nov 2010; published 1 Dec 2010

opposite sign. This technique, however, requires a long-arm interferometer because it must use the AOM diffraction effect, bringing with it the disadvantages of a two-arm *f*-2*f* interferometer in addition to increased system complexity. Recently, a direct and simple method for generating identical CEP pulses, known as the "direct locking" (DL) method, was demonstrated by the authors [8,9]. This technique maintains CEP without using radio frequency equipments and optical elements such as a referenced local oscillator and an AOM. With this advantage, the DL method can be used in combination with a common-path interferometer for further improvements to the stability and long-term coherence of CEP due to its compact setup and because it is capable of generating identical pulses.

In this present study, the long-term CEP coherence of a femtosecond laser with zero pulse-to-pulse phase slip, achieved by the DL method, is demonstrated by utilizing a quasi-common-path interferometer (QPI) in a compact Michelson setup. To evaluate the stability of the stabilized CEP, the noise properties of CEP error signals obtained with a two-arm *f*-2*f* interferometer and QPI setups are compared. From the CEP error signals, the phase power spectral density (PSD) technique in the frequency domain and the integrated phase timing jitter and Allan deviation in the time domain are calculated and compared. With improved CEP stability, the long-term phase coherence of CEP is measured for more than 56 hours with an accumulated phase noise well below 1 radian. In addition, the phase fluctuation property is analyzed from the modified Allan deviation. From this result, the relative stability is estimated to be approximately 1.4×10^{-22} at 790 nm. This is a much improved result compared to our earlier work on long-term CEP stabilization [15], or to a result achieved by other group [16].

2. CEP stabilization

A femtosecond laser oscillator operated at 80 MHz with a central wavelength at 790 nm is a typical mode-locked femtosecond Ti:Sapphire laser. For one octave broadening of the spectrum through nonlinear processes, a photonic crystal fiber (PCF) is used at each of in-loop and out-of-loop setups. CEP stabilization of the femtosecond laser is achieved by the DL scheme with a balanced detection setup. As the experimental details of the DL technique are available in the literature [8,9], only a brief description is provided here. The beat signals obtained from the *f*-2*f* interferometer are sent to a balanced photodiode (BPD) to obtain the signal containing CEP variation. The pure CEP signal is extracted from the interferometer beat signal after the direct current term is eliminated by BPD. In this study, CEP is stabilized both by changing the power of the pumping laser using an AOM and by controlling the insertion of a dispersion-compensation prism in the femtosecond oscillator cavity with a piezo-electric transducer for long-term CEP stabilization. The mixing product technique or a lock-in amplifier measurement technique is not necessary to obtain CEP fluctuations for measuring PSD, because the CEP signal itself is used as a phase error signal in near-zero frequency.

For a comparison of the stability performance, a QPI and a two-arm *f*-2*f* interferometer were constructed, as shown in Fig. 1. First, two Mach-Zehnder (MZ) setups are installed to measure the CEP signal in the in-loop (lower part in blue dashed box) and out-of-loop (upper part in blue dashed box) conditions, as shown in Fig. 1. The octave-broadened spectrum is separated into two paths by a dichroic beam splitter. The low-frequency component of the spectrum around 1064 nm is frequency-doubled by a KTP crystal and overlapped with the high-frequency component around 532 nm with an adjustable time delay.

#136419 - $15.00 USD Received 11 Oct 2010; revised 24 Nov 2010; accepted 28 Nov 2010; published 1 Dec 2010

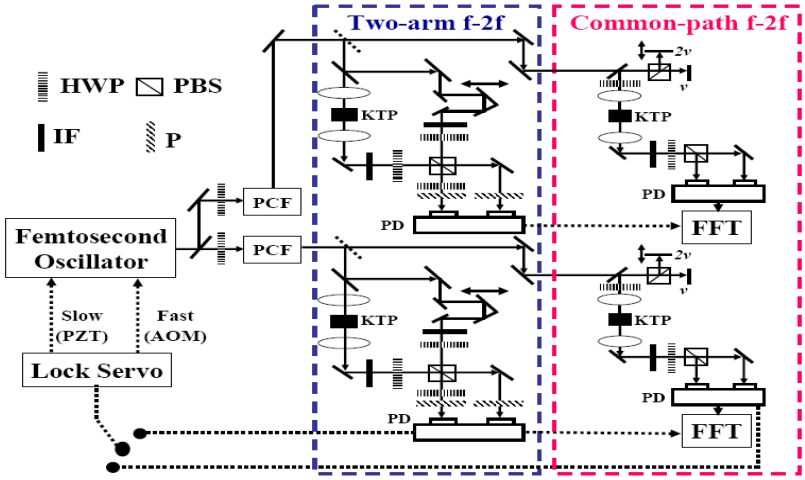

Fig. 1. (Color online) Experimental setup used for comparing the stability performance between a two-arm *f*-2*f* interferometer (blue dashed box) and a quasi-common-path *f*-2*f* interferometer (red dashed box). The in-loop interferometer and DL setup are used to stabilize the CEP of the femtosecond laser, and the out-of-loop interferometer serves to monitor the stability performance of CEP. The black lines and dashed lines denote the paths of optical and electrical signals, respectively. FFT: fast Fourier-transform analyzer, HWP: half-wave plate, IF: interference filter, P: polarizer, PBS: polarization beam splitter, PCF: photonic crystal fiber, PD: double balanced detector, PZT: piezo-electric transducer.

The beat signal in the MZ interferometers is measured with a fast photodiode, obtaining a signal-to-noise ratio higher than 35 dB with a 300 kHz resolution bandwidth in the in-loop and out-of-loop conditions. In order to estimate the stability of CEP, the PSD is measured in both the in-loop and out-of-loop conditions using a fast Fourier-transform (FFT) analyzer.

As the second setup for comparison and improvement of CEP stability, a QPI in a simple Michelson setup is used instead of the two-arm interferometer setup, in the in-loop (lower part) and out-of-loop (upper part) conditions, as shown in the red dashed box in Fig. 1. This simple structure nullifies the effects of external perturbations such as vibration and acoustic noise. The compact Michelson interferometer is used to control the group delay mismatch between the high-frequency component and the frequency-doubled low-frequency component, and a half-wave plate is inserted to adjust the polarization to obtain optimum second harmonic conversion. The high-frequency and low-frequency components are separated and combined by a polarizing beam splitter that works well even with a coating for the wavelength at 532 nm. The Michelson interferometer used in the QPI scheme is useful because its simple configuration can be accommodated without a broadband spectral coating and the thin thickness required in the case of a harmonic separator [17–19]. In order to avoid an optical loss, different beam heights are used before and after the Michelson interferometer. With this QPI scheme, a beat signal with a contrast of mort than 35 dB is obtained. A FFT analyzer is also used to measure the phase fluctuations of the stabilized CEP.

3. CEP stability

The noise properties of the stabilized CEP in the two interferometer schemes were investigated to improve the CEP stability. To estimate the CEP stability, the power spectral density technique and the Allan deviation method were utilized. Phase fluctuations (or phase modulation noise) in the frequency domain are frequently evaluated by the PSD, and the fractional frequency stability of a signal in the time domain can be characterized by the Allan deviation.

#136419 - $15.00 USD Received 11 Oct 2010; revised 24 Nov 2010; accepted 28 Nov 2010; published 1 Dec 2010

3.1 Comparison of phase noises in two f-2f interferometers

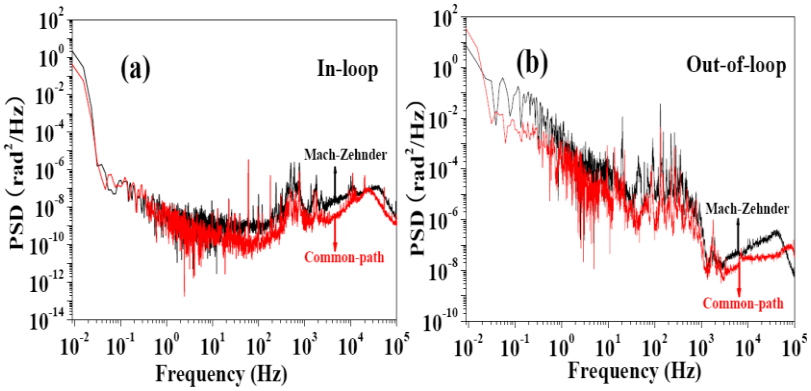

Fig. 2. (Color online) Phase power spectral density of stabilized CEP signals obtained with two interferometer setups in in-loop (a) and out-of-loop (b) conditions. The black lines represent the results of the two-arm *f*-2*f* interferometer and the red lines represent those of the quasi-common-path *f*-2*f* interferometer.

The phase error signal of the stabilized CEP can be coupled to a FFT analyzer that measures the root-mean-square (rms) voltage $V_{\mathrm{rms}}(f)$ of phase fluctuation at Fourier frequency *f*. The PSD of CEP noise is given by the equation

$$S_{\phi}(f) = \left\{ \frac{V_{\mathrm{rms}}(\mathrm{f})}{V_{\mathrm{s}}} \right\}^{2} \frac{1}{BW}, \tag{1}$$

where V_s is the sensitivity (V/rad) of a phase detector, and BW is measurement bandwidth [20,21]. In this study, a balanced photodiode plays the role of the phase detector in near-zero frequency. The stability of CEP is compared in terms of its frequency domain phase noise in in-loop and out-of-loop conditions, as shown in Fig. 2. In Figs. 2(a) and 2(b) PSDs obtained with the two-arm interferometer and with the QPI are shown as black and red curves, respectively. In the in-loop results shown in Fig. 2(a), the dominant noise components are white phase noise, varying as f^{0}, as clearly illustrated by the frequency dependency of PSDs. This is a consequence of CEP stabilization by the DL method using a pure phase signal. In the in-loop condition, the strong phase noise measured in the frequency band from 300 Hz to 800 Hz stems from the amplitude-to-phase conversion noise in the PCF caused by environmental effects such as acoustic noise, air pressure, and mechanical vibration [22–24]. With the QPI, the phase noise is significantly improved at frequencies above 10 Hz, confirming that the QPI is less sensitive to environmental perturbations than the two-arm interferometer.

Figure 2(b) shows the phase noise comparison result between the two interferometers in the out-of-loop condition. Flicker phase noise, varying as f^{-1} in the PSD, can be seen for the frequency below 10 Hz in both black and red curves. Because this type of noise is related to mechanical vibrations and temperature fluctuation at the low-frequency region, it can be explained as a drift of the *f*-2*f* interferometer due to environmental effects [11,12]. Strong fluctuations of phase noise are also observed in the frequency band from 10 Hz to 800 Hz due to amplitude-to-phase noise conversion in PCF, similarly to those seen in Fig. 2(a). When compared to the in-loop noise, the out-of-loop phase noise contains extra contributions coming from uncompensated noises generated in the out-of-loop *f*-2*f* interferometer and also in PCF. Flicker frequency noise, varying as f^{-3} in the PSD, is observed in the frequency band from 800 Hz to 2 kHz in both cases. The physical cause of this noise may be related to environmental perturbations [20,21]. This noise appears only in the out-of-loop condition because the electrical feedback loop in-loop works to cancel it. In this measurement, the upper

#136419 - $15.00 USD Received 11 Oct 2010; revised 24 Nov 2010; accepted 28 Nov 2010; published 1 Dec 2010

limit of phase noise measurement is set to be 102 kHz, as determined by the maximum bandwidth of the FFT analyzer, although the range of integration should be up to the Nyquist frequency ($f_{rep}/2 \approx 40$ MHz) [18,19]. For most frequency ranges, the phase noise of the QPI scheme is much improved over that of the two-arm system; the QPI scheme can significantly reduce the interferometer drift - a major factor in CEP drift.

3.2 Integrated phase timing jitter and Allan deviation

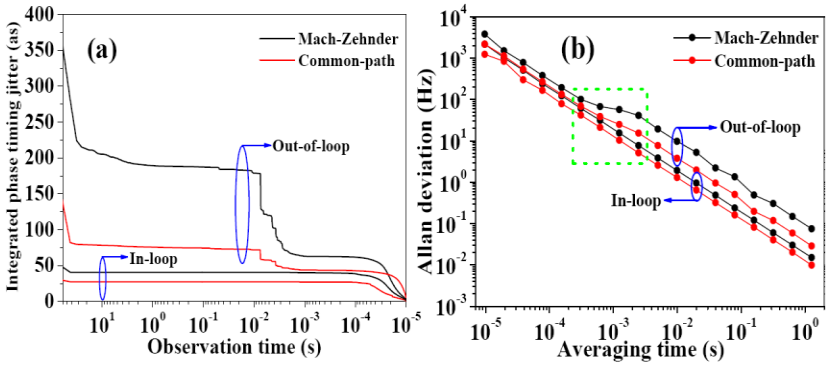

Fig. 3. (Color online) (a) Integrated phase timing jitter and (b) Allan deviation calculated from the phase power spectral density given in Fig. 2. The black line and red line represent the results obtained with the two-arm scheme and the quasi-common-path scheme, respectively.

To evaluate the stability of CEP in the time domain, the integrated phase timing jitter and the Allan deviation are calculated by integrating the PSDs measured in both the in-loop and out-of-loop conditions. The black and red lines in Fig. 3 represent the results obtained with the two-arm interferometer and the QPI, respectively. The phase timing jitter, corresponding to the PSD in Fig. 2, is calculated as a function of the observation time. This is presented in Fig. 3(a). The rms accumulated phase timing jitter (ΔT_{rms}) is defined as

$$\Delta T_{rms}(\tau_{obs}) = \frac{\lambda_C}{2\pi c}\Delta\phi_{rms}(\tau_{obs}) = \frac{\lambda_C}{2\pi c}\left\{2\int_{1/\tau_{obs}}^{\infty} df\, S_\phi(f)\right\}^{\frac{1}{2}}, \quad (2)$$

where $\Delta\varphi_{rms}$ and τ_{obs} denote the integrated phase error and observation time, respectively, and λ_C and $S_\varphi(f)$ represent the central wavelength of the laser pulses and the PSD, respectively [11–13]. When the CEP is stabilized with pure phase error signals at zero frequency, the integrated rms phase noise of CEP can be interpreted as the deviation of phase fluctuation at the observation time. The coherence time is also defined by the integration of the PSD $S_\varphi(f)$ up to the observation time at which the accumulated phase error $\Delta\varphi_{rms}$ becomes 1 radian [22]. The comparison of the phase timing jitters in-loop clearly shows the improved performance of the QPI scheme. The accumulated phase noise of the in-loop QPI, for an observation time ranging from 10 μs to 60 s, is approximately 66 mrad. The corresponding integrated phase timing jitter is 27 attoseconds at 790 nm, as shown in Fig. 3(a). In the out-of-loop condition, the phase timing jitter of the QPI scheme is reduced by more than 2 times when compared to that of the two-arm scheme. This result clearly shows that the QPI scheme is much more suitable for long-term CEP stabilization compared to the two-arm scheme. Several step increases are observed in the out-of-loop phase timing jitter, coming mostly from the amplitude-to-phase conversion noise in PCF and long non-common path length in two-arm *f*-2*f* interferometer. The QPI scheme contains much smaller steps than the two-arm scheme, indicating that the two-arm *f*-2*f* interferometer is more sensitive to environmental effects compared to the QPI.

The stability of CEP was also estimated with the Allan deviation ($s_y(t)$), as shown in Fig. 3(b). The black and red circle lines in Fig. 3(b) denote the Allan deviation obtained with

#136419 - $15.00 USD Received 11 Oct 2010; revised 24 Nov 2010; accepted 28 Nov 2010; published 1 Dec 2010

the two-arm interferometer and with the QPI, respectively. The Allan deviation, derived from the PSD in Fig. 2, is given by the following equation:

$$\sigma_y(\tau) = \left\{ \frac{2}{(\pi \nu_0 \tau)^2} \int df\, S_\phi(f) \sin^4(\pi f \tau) \right\}^{\frac{1}{2}} \quad (3)$$

Here, t and ν_0 are the averaging time and the carrier frequency, respectively [20,21]. In the in-loop condition, the Allan deviation of the QPI scheme is 9.9×10^{-3} Hz at an averaging time of 1 second. Here, the unit of the Allan deviation is given in Hz, because the nominal frequency of CEP-stabilized laser pulses operates at zero frequency. The slope of the Allan deviation decreases inversely to the averaging time in both the in-loop and out-of-loop conditions, implying that white phase noise contributes mostly to the CEP fluctuations. This result is expected in Fig. 2, because the CEP is stabilized by a pure CEP signal in the case of the DL method operating at zero frequency. The short-term stability improved by the QPI scheme is directly attributed to the reduced phase noise of Fig. 2, as shown in Fig. 3(b). It was noted that the flicker frequency noise, varying as t^0 to the averaging time, is enhanced in the out-of-loop measurement in the range from 6×10^{-4} to 2.5×10^{-3} s (marked with the green dashed box). The smaller signal for the QPI scheme also indicates that the CEP stabilization achieved with the QPI scheme is less affected by environmental effects.

3.3 Long-term carrier-envelope phase coherence

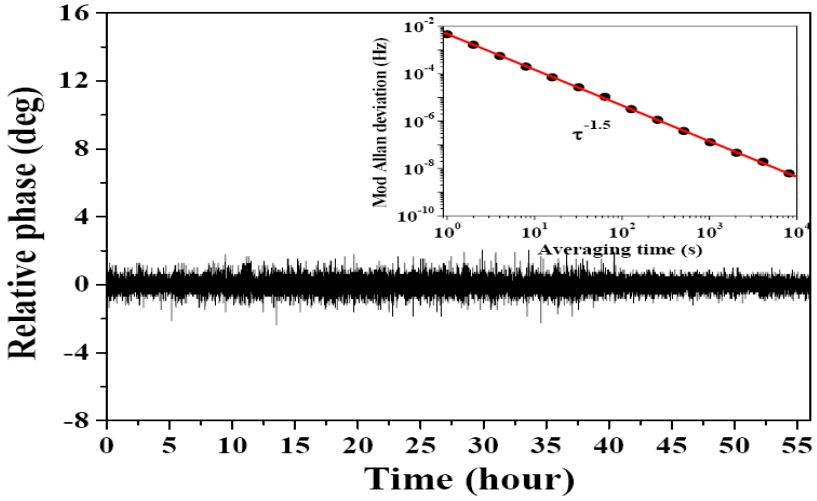

Fig. 4. (Color online) In-loop beat signal observed over two days while maintaining CEP stabilization. The rms accumulated phase noise was calculated to be 60 mrad, which corresponds to a phase time jitter of 25 attoseconds at a central wavelength of 790nm. The inset shows the modified Allan deviation calculated with the long-term stabilized signal.

With the phase noise improvement achieved by employing the QPI scheme, long-term maintenance of the stabilized CEP is examined. Figure 4 shows the results of long-term stabilized CEP signals obtained at in-loop with the QPI scheme. It is important to note that this result was achieved without realignment of any optical components for more than two days. The rms accumulated phase noise of the CEP error signal was measured to be approximately 60 mrad, which corresponds to a phase timing jitter of 25 attoseconds at 790 nm. This result is a clear demonstration that CEP coherence can be preserved for 56 hours, as the accumulated phase fluctuation remains well below 1 radian. This result is in good agreement with the result of the integrated phase timing jitter measured in-loop, as shown in Fig. 3(a). The relative timing stability of CEP was calculated to be approximately 1.4×10^{-22}, which is derived by dividing the integrated phase timing jitter with the total time of the

#136419 - $15.00 USD Received 11 Oct 2010; revised 24 Nov 2010; accepted 28 Nov 2010; published 1 Dec 2010

stabilized CEP. For further verification of the maintenance of CEP coherence, the modified Allan deviation was calculated from the long-term phase fluctuation signals. The modified Allan deviation technique is employed to clarify the stability estimation of a source. Depending on the type of noise that dominates, the modified Allan deviation behaves as $\tau^{-1.5}$ for white phase noise, or τ^{-1} for flicker phase noise [20,21]. The modified Allan deviation, shown by the red curve in the inset of Fig. 4, behaves as $\tau^{-1.5}$ to the averaging time, indicating that the CEP noise is governed by white phase noise. The modified Allan deviation at an averaging time of 1 s was found to be 4.5×10^{-3} Hz, which shows good agreement with the Allan deviation value at in-loop in Fig. 3(b). This is a clear indication that short-term and long-term stability levels are managed by the same noise process. From this result, it can be confirmed that the major noise source contributing to the stability of the CEP is white phase noise, which does not lead to an accumulation of phase fluctuations. As a consequence, CEP coherence is preserved for more than 56 hours, showing that the phase coherence is maintained without phase cycle slip for more than 1.6×10^{13} pulses. Consequently, the long-term CEP coherence of laser pulses with identical CEP values has been achieved by coupling a QPI with the DL method used for the CEP stabilization of a femtosecond laser. As the current long-term CEP stabilization is demonstrated with standard optical components, not using specially designed optics such as ultra-broadband chirped mirrors [18], Wallaston prism pairs [11], or thin harmonic separator [17] for the adjustment of very wideband group delay, the present QPI can be easily adopted in any CEP stabilization scheme, providing high practicality. This can also serve as a functional tool in metrological applications such as physical constant measurements or an optical lattice clock work.

4. Conclusion

The long-term CEP coherence of a femtosecond laser with CEP stabilized by the DL method is demonstrated using a QPI. CEP stability in two different interferometer setups is compared by measuring the PSD in the frequency domain and the integrated phase timing jitter and the Allan deviation in the time domain. These results clearly show that the QPI scheme is more stable than the two-arm scheme as the former is not sensitive to environmental perturbations due to the short separated path lengths of the QPI. The stability of CEP improved by the QPI scheme primarily contributes to maintaining long-term CEP coherence for more than 56 hours. To confirm the CEP coherence in a long-term scale, the modified Allan deviation, calculated from the long-term CEP signal, shows that the phase timing jitter of the CEP is entirely due to white phase noises, indicating that the CEP coherence is preserved for a long period. As a consequence, few-cycle femtosecond pulses with long-term CEP coherence, achieved by the direct locking method coupled with the QPI, will greatly benefit attosecond physics and frequency metrology.

Acknowledgements

This work was supported by the Ministry of Education, Science, and Technology of Korea through the National Research Foundation.

#136419 - $15.00 USD Received 11 Oct 2010; revised 24 Nov 2010; accepted 28 Nov 2010; published 1 Dec 2010